Supplement of Earth Surf. Dynam., 12, 727–745, 2024
https://doi.org/10.5194/esurf-12-727-2024-supplement

Earth Surface Dynamics
Open Access
EGU

Supplement of

Stream hydrology controls on ice cliff evolution and survival on debris-covered glaciers

Eric Petersen et al.

Correspondence to: Eric Petersen (eipetersen@alaska.edu)

S1. Introduction

This supporting material contains text, video, figures, and tables, summarizing additional information on ice cliff backwasting ramp selection sensitivity analysis (Text S1), stream identification (Figure S1), ice cliff DEM analysis (Figures S2-S3), discharge measurements (Figures S4-S8, Table S1), time lapse videos of stream avulsion events (Videos S1-S2), and an animation of ITS_LIVE glacier velocity data (Video S3).

S2. Geomorphic Model Sensitivity Analysis

We assessed the sensitivity of our ice cliff backwasting ramp geomorphic analysis to topographic profile selection by comparing the results of many different sample locations along the length of two ice cliffs (one each with and without associated supraglacial streams). 12 profiles were extracted along the ice cliff with no stream (~35 m in length) and 16 profiles were extracted along the ice cliff with an associated stream (~73 m in length). These profiles were analyzed following our geomorphic model of ice cliff backwasting (Main Text, Section 3.3; Figure S2).

The determined values of ψ, which indicates the angle between the ice cliff and its backwasting ramp, exhibited a standard deviation of 5.2° for the stream-affected cliff (range of 110-129°) and 3.3° for the non-stream-affected cliff (range of 144-154°). Standard deviations of the ramp and ice cliff angles include 3.0° and 3.3° for the stream-affected cliff and 1.9° and 2.0° for the non-stream-affected cliff, respectively.

From this analysis we thus estimate the uncertainty due to topographic profile selection on the results of our geomorphic model as $\pm$ 3° for ice cliff and backwasting ramp angles and $\pm$ 5° for the angle ψ between ice cliff and backwasting ramps.

S3. Description of Supplementary Videos

Supplementary Video 1 is a time lapse video of Avulsion #1 in action (described in Figures 8 & 11 of the main text). Frame interval is 30 minutes. Note the ablation stake in the foreground melting out of debris-covered ice.

Supplementary Video 2 is a time lapse video of Avulsion #2 in action (described in Figures 8 & 11 of the main text). Frame interval is 30 minutes.

Supplementary Video 3 is a data animation illustrating results from the ITS_LIVE glacier velocity dataset on Kennicott Glacier. This velocity data was generated using auto-RIFT (Gardner et al., 2018) and provided by the NASA MEaSUREs ITS_LIVE project (Gardner et al., 2022). (a) Velocity field on Kennicott Glacier mapped through time. (b-f) Velocity profiles extracted from the map; y axis is in m annum^{-1} and x axis is in m. Red line indicates the current year while previous years are underplotted in progressively

transparent black lines going into the past. Two readvances are observed in the vicinity of the (e) profile, circa 1988-1995 and 2018-2020.

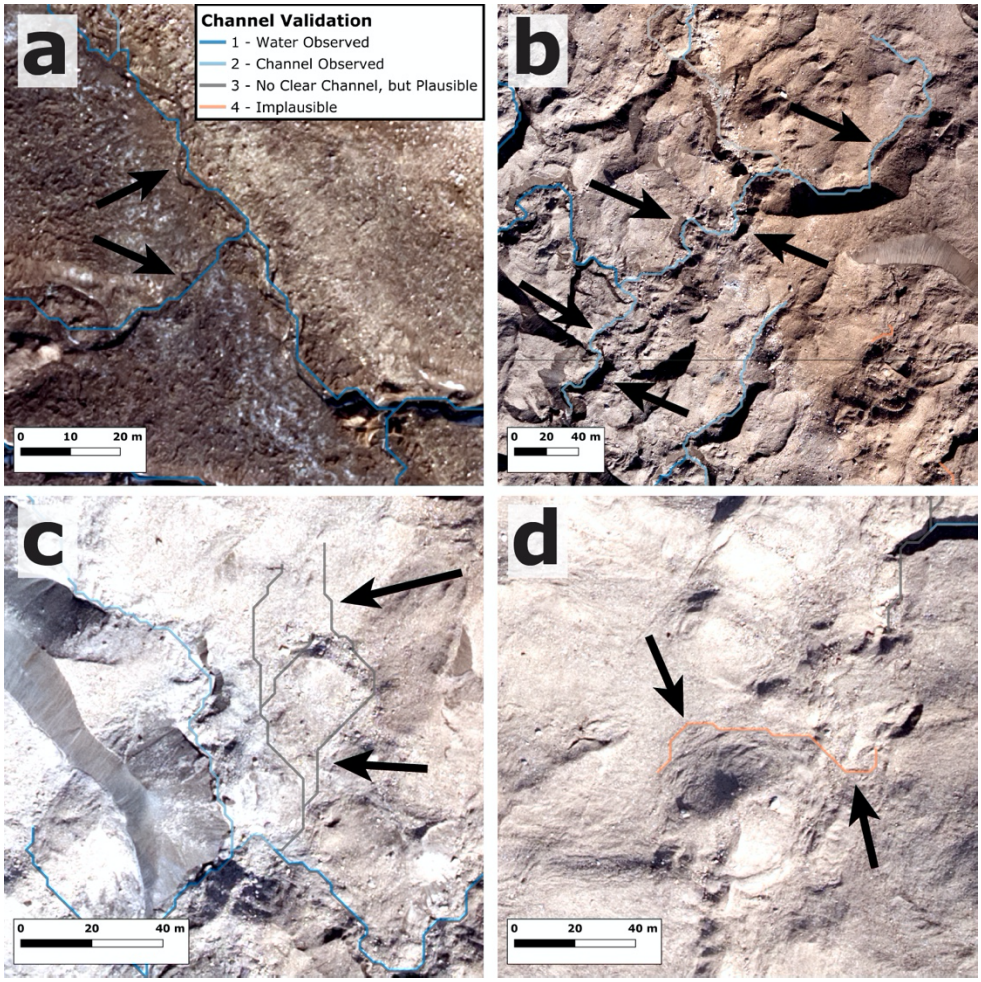

Figure S1: Examples from stream channel validation of (a) active water flow observed in candidate channels, (b) channel morphology observed with no confirmed water, (c) no clear channel morphology but other signs of hydrologic activity (association to ponds/channels, textured debris, dendritic network, (d) clearly no significant hydrologic activity.

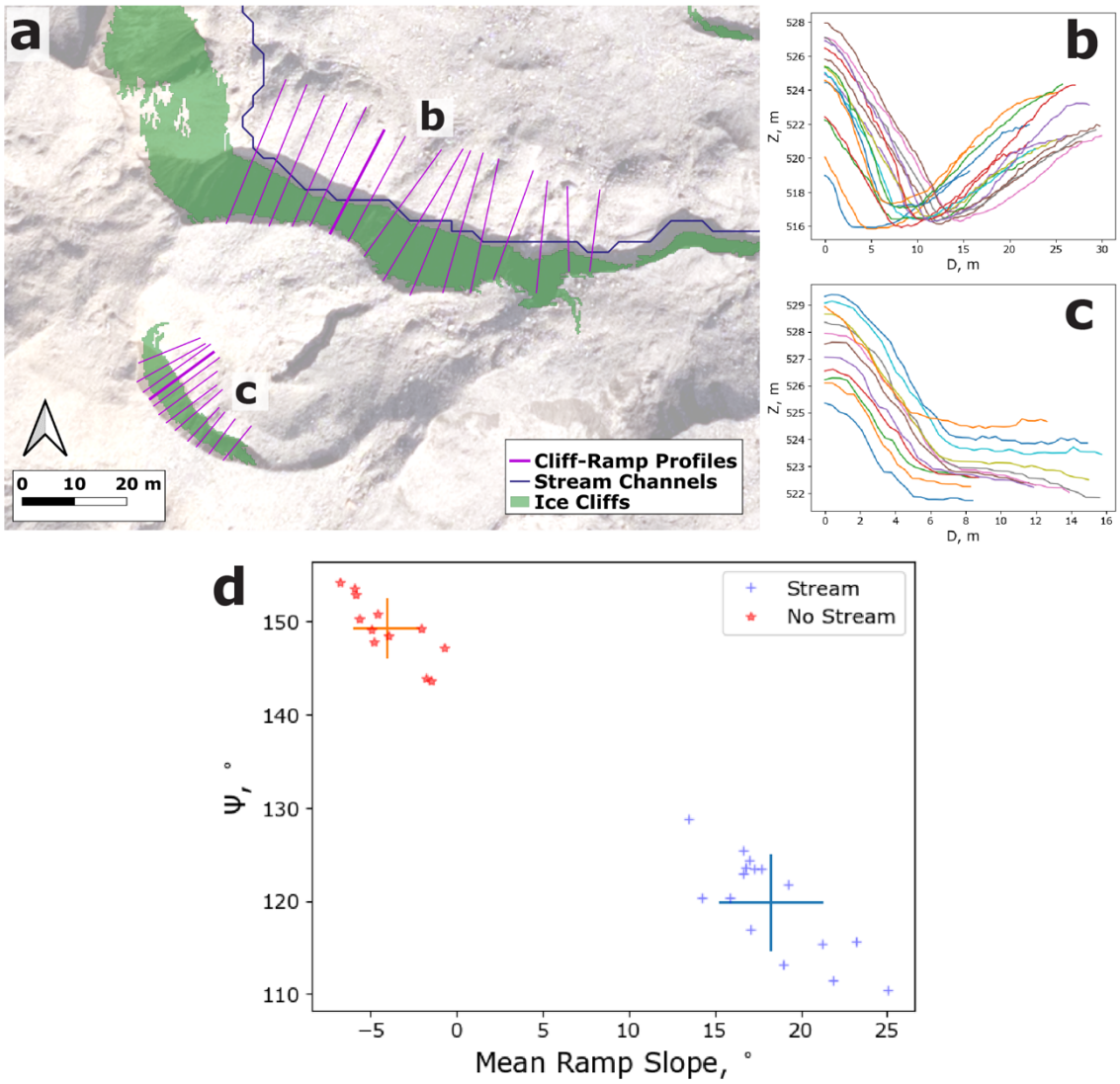

Figure S2: Sensitivity analysis of topographic profile location selection on results for ice cliff-ramp systems with and without associated supraglacial streams. (a) Map of ice cliffs used in sensitivity analysis, with NPS orthophoto used as the basemap. (b) All profiles extracted from the ice cliff associated with a supraglacial stream. (c) All profiles extracted from the ice cliff with no associated stream. (d) Constrained ψ value (angle difference between mean ice cliff and backwasting ramp slopes) plotted against mean ramp slope for each of the profiles selected on the ice cliffs with and without associated supraglacial streams. Individual measurements are shown as symbols; error bars illustrate the mean and standard deviation of each population.

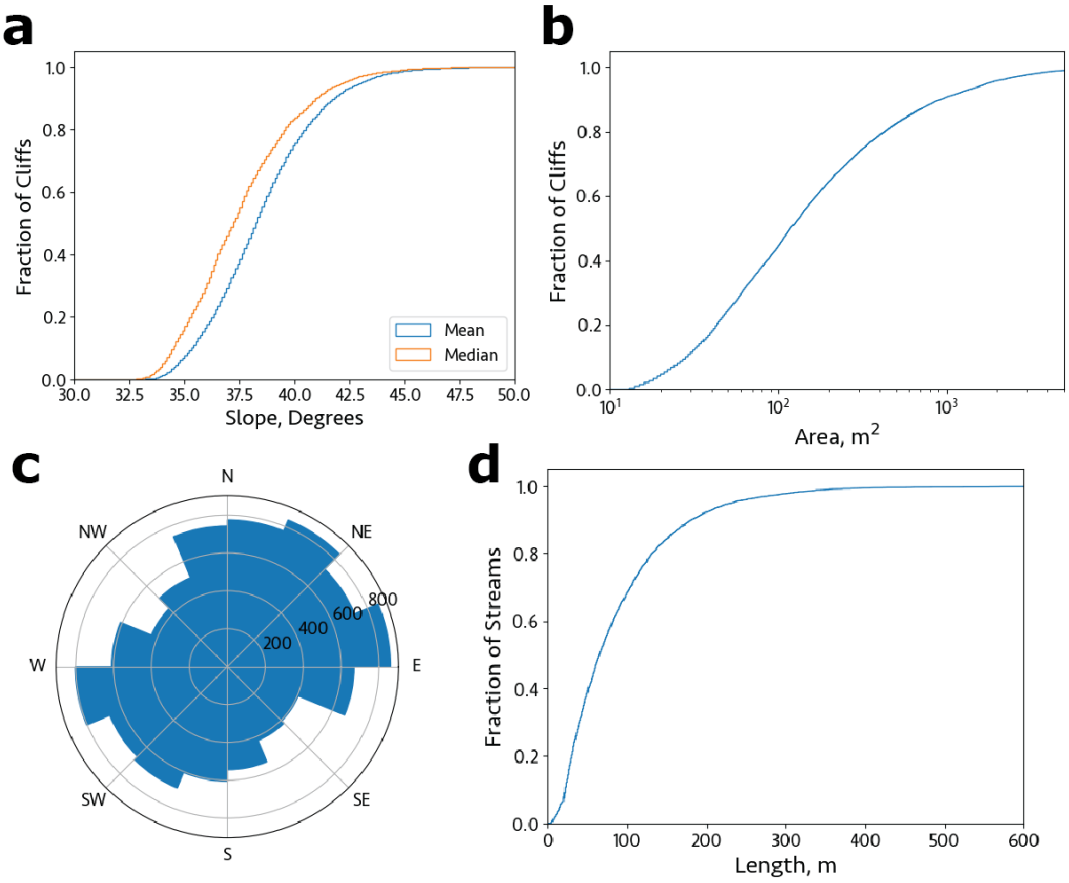

Figure S3: Cumulative statistics on ice cliff (a) surface slope, (b) geometric area and (c) aspect as well as (d) supraglacial stream length. Ice cliff metrics represent median values for ice cliff shapes, not raw pixel values.

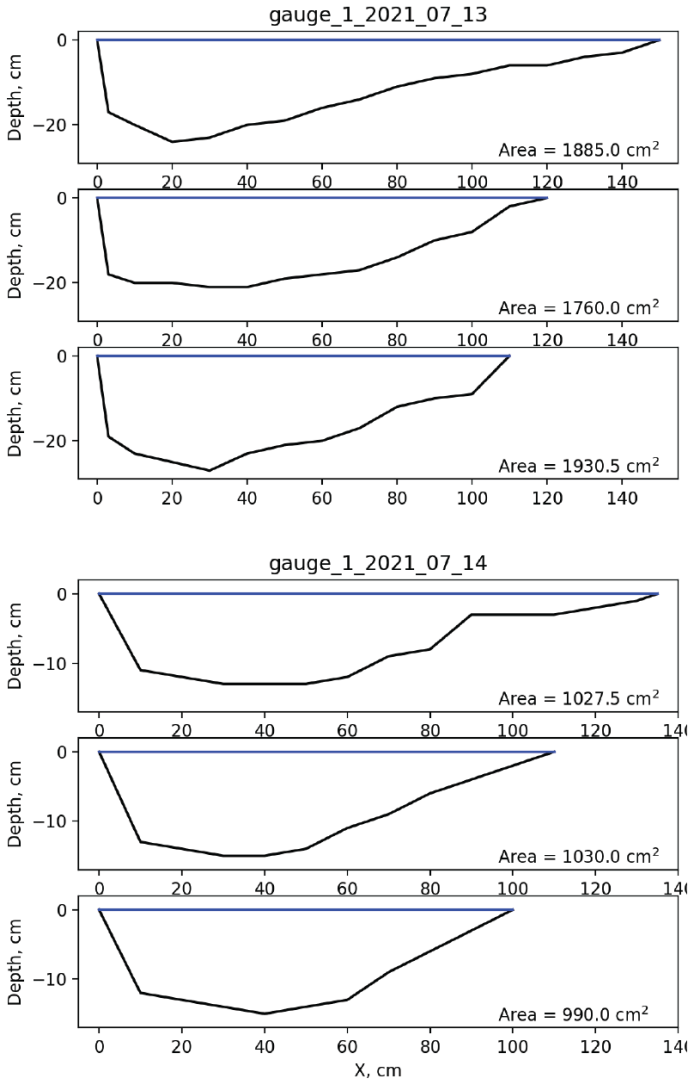

Figure S4: Measured channel cross-sections for stream discharge measurement 1. The ice cliff face is located at 0 cm on each profile.

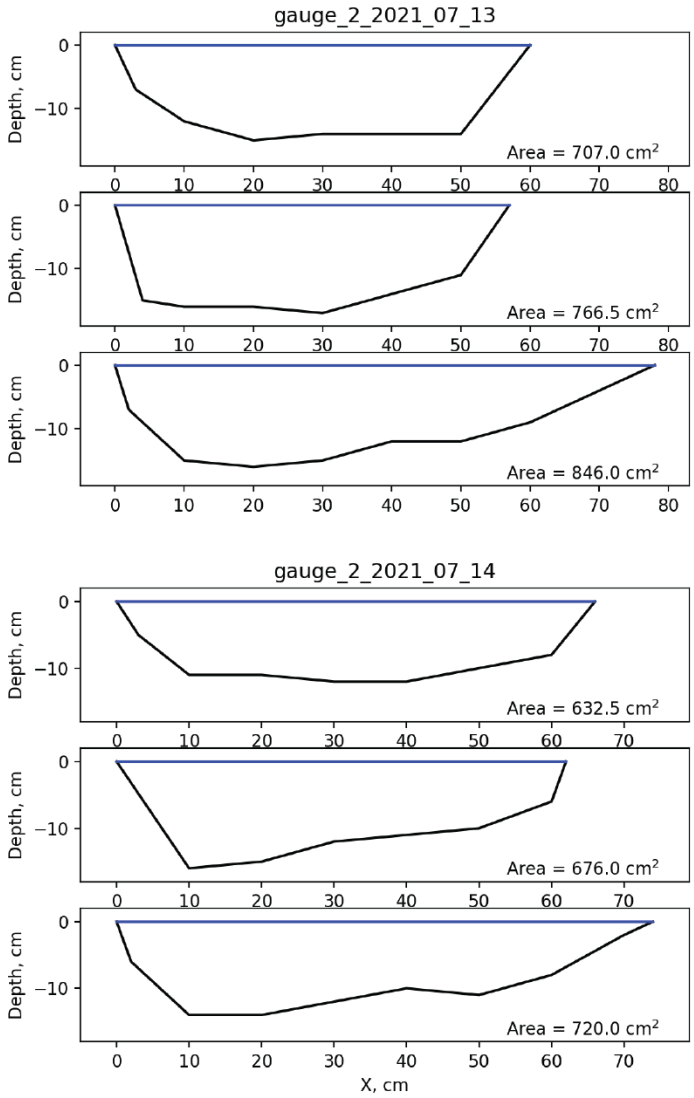

Figure S5: Measured channel cross-sections for stream discharge measurement 2. The ice cliff face is located at 0 cm on each profile.

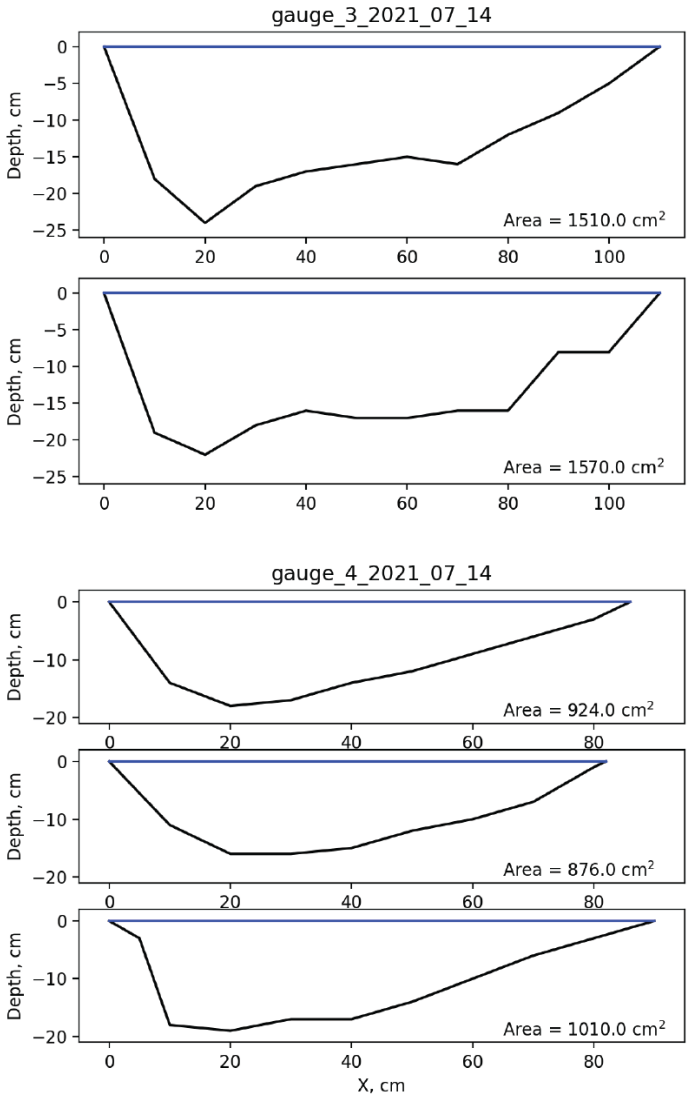

Figure S6: Measured channel cross-sections for stream discharge measurements 3-4. The ice cliff face is located at 0 cm on each profile.

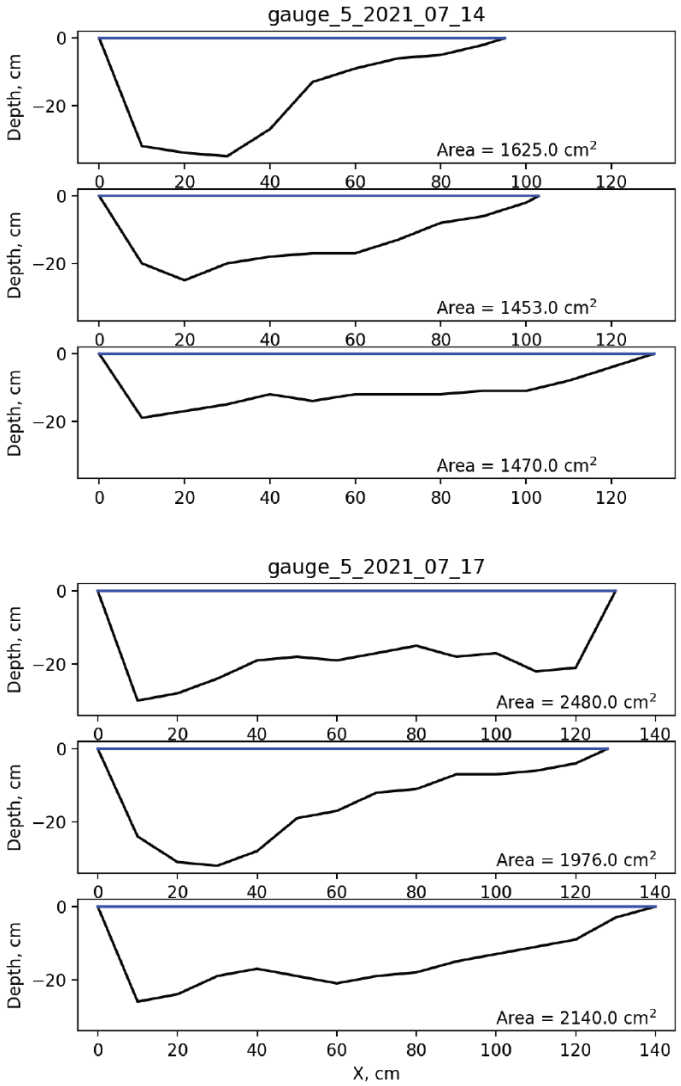

Figure S7: Measured channel cross-sections for stream gauge 5. The ice cliff face is located at 0 cm on each profile.

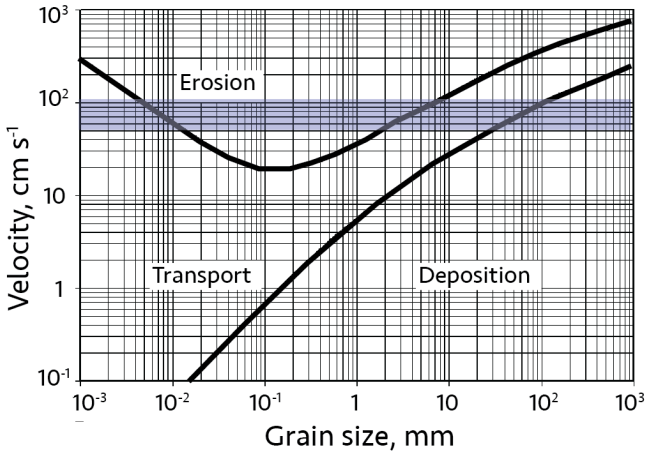

Figure S8: Hjulström curve (Hjulström, 1935) with velocities constrained from supraglacial stream discharge measurements overplotted in blue shading.

Gauge	Date	Time	Conditions	Length (m)	Datapoints	Latitude	Longitude	Z	Velocity (m/s)	Area (cm^2)	Flow (m^3/s)
1.1	July 13, 2021	~3:20-3:45 PM	Hot, sunny	8	8	61.4833	-142.9169	551.6	0.6	1700	0.102
1.2	July 14, 2021	2:32 PM	Cool, cloudy	8	6	61.4833	-142.9169	551.6	0.6	950	0.057
2.1	July 13, 2021	~3:50-4:15 PM	Hot, sunny	5	5	61.4836	-142.9161	553.5	1.1	700	0.077
2.2	July 14, 2021	~12:00 PM	Cool, cloudy	4	8	61.4836	-142.9161	553.5	0.9	611	0.055
3.1	July 14, 2021	~3:30 PM	Cool, cloudy	1.5	15	61.4822	-142.9144	530.5	0.8	1413	0.113
4.1	July 14, 2021	~4:00 PM	Cool, cloudy	6	8	61.4829	-142.9156	543.3	1.0	850	0.085
5.1	July 14, 2021	4:24 PM	Cool, cloudy	3	7	61.4828	-142.9154	544.9	0.9	1389	0.125
5.2	July 17, 2021	1:30-1:50 PM	Hot, sunny	2.5	7	61.4828	-142.9154	544.9	1.0	1850	0.185

Table S1: Summary of stream gauging experiments conducted on Kennicott Glacier for this study. Median velocity, channel cross-sectional area, and flow rates as constrained by the experiments are shown.